5

Sterile dark matter, baryogenesis and neutrinoless double beta decay in a $A_4 \otimes Z_8$ based ν2HDM

We discuss the impact of neutrino phenomenology and related cosmology on a $A_4 \otimes Z_8$ symmetric ν2HDM along with an addition of a new particle, i.e. a gauge singlet (S). The additional particle is a sterile neutrino which is considered to be a probable dark matter candidate in our work. With the choice of sterile neutrino mass in keV range we evaluate the active-DM mixing angle, decay rate and relic abundance considering various cosmological constraints. Simultaneously, a detailed analysis on baryogenesis and neutrinoless double beta decay is also carried out for low scale right-handed neutrino masses. We have considered various bounds from experiments such as Lyman-α, X-ray observation, Planck data and KamLAND-Zen limit to validate the model w.r.t the phenomena studied in it.

5.1 Introduction

In the Minimal Extended seesaw (MES), which is an extension of the canonical type-I seesaw, three additional right handed neutrinos and one gauge singlet chiral fermion field S as a sterile neutrino are included to the standard model particles. In this formalism, the 4×4 active-sterile neutrino mass matrix is given by

$$M_\nu^{4\times4} = -\begin{pmatrix} M_D M_R^{-1} M_D^T & M_D M_R^{-1} M_S^T \\ M_S (M_R^{-1})^T M_D^T & M_S M_R^{-1} M_S^T \end{pmatrix} \tag{5.1}$$

where M_D, M_R and M_S are the Dirac, Majorana and Sterile neutrino mass matrices. Now the light neutrino mass matrix can be written as, [97]

$$M_\nu^{3\times3} \simeq M_D M_R^{-1} M_S^T (M_S M_R^{-1} M_S^T)^{-1} M_S (M_R^{-1})^T M_D^D - M_D M_R^{-1} M_D^T \tag{5.2}$$

and the sterile neutrino mass as,

$$m_s \simeq -M_S M_R^{-1} M_S^T \tag{5.3}$$

Neutrinos with sub-eV scale are obtained from M_D at electroweak scale, M_R at TeV scale and M_S at keV scale.

Motivated by the shortcomings of the Standard Model, we have done a phenomenological study on the neutrino two Higgs doublet model (ν2HDM) in the framework of Minimal Extended Seesaw in which the particle content of SM is extended by a new Higgs doublet field (η), three singlet neutral fermions (N_i) and one sterile singlet neutrino (S). We have constructed the Dirac mass matrix in such a way that the $\mu - \tau$ symmetry is broken to generate the non-zero reactor mixing angles. We calculate the effective neutrino mass using the global fit analysis data in the 3σ range and studied its variation with lightest neutrino mass and compared the value of effective mass with KamLAND-Zen bouds both in NH and IH cases. We have studied the DM phenomenology considering the lightest sterile

neutrino (S) as a potential DM candidate. We have evaluated the model parameters and then calculated DM mass, DM active mixing, relic density and the decay rate of the sterile neutrino. We have basically discussed the impact of neutrino phenomenology and related cosmology on a $A_4 \otimes Z_8$ symmetric ν2HDM along with an addition of a new particle, i.e. a gauge singlet (S). With the choice of sterile neutrino mass in keV range we evaluate the active-DM mixing angle, decay rate and relic abundance considering various cosmological constraints. Simultaneously, a detailed analysis on baryogenesis and neutrinoless double beta decay is also carried out for low scale right-handed neutrino masses. We have considered various bounds from experiments such as Lyman-α, X-ray observation, Planck data and KamLAND-zen limit to validate the model w.r.t the phenomena studied in it. This paper is organized as follows. In section (5.2) we have discussed the generic ν2HDM following the $A_4 \otimes Z_8$ model and generation of the mass matrices in the leptonic sector. Section (5.3) includes discussion on sterile dark matter and the constraints from X-ray and Lyman-α. In section (5.4), we discuss leptogenesis generated in this model. Numerical analysis and results are discussed in section (5.5). Finally, the summary of our work is concluded in section (5.6).

5.2 $A_4 \otimes Z_8$ realization of extended ν2HDM

It will not be natural if we consider that the neutrino mass comes from the SM Higgs doublet (H) as the neutrino Yukawa coupling constant is too small compared to other leptons and quarks. This problem can be solved if we consider that the neutrino mass comes from another scalar doublet with naturally small vacuum expectation value (vev). ν2HDM model[71] is one of the natural choices for beyond SM models containing two Higgs doublets instead of just one.

Consider the minimal Standard Model with three lepton families:

$$\begin{pmatrix} \nu_i \\ l_i \end{pmatrix}_L \sim (1,2,-1/2), l_{iR} \sim (1,1,-1)$$

Now we add three neutral fermion singlets, $N_{iR} \sim (1,1,0)$. We assign them $L=0$ instead of $L=1$ to forbid the Yukawa coupling term with SM Higgs doublet. Now we introduce a new scalar doublet η as,

$$\begin{pmatrix} \eta^+ \\ \eta^0 \end{pmatrix} \sim (1,2,1/2)$$

with $L=-1$.

The new Yukawa interaction and mass terms are:

$$-\mathcal{L}_Y \sim y\bar{L}\tilde{\eta}N + \frac{1}{2}\bar{N^c}m_N N + h.c. \tag{5.4}$$

Here, $\tilde{\eta} = i\sigma_2\eta^*$ and the lepton number is violated by 2 units in the first term of the Yukawa interaction Lagrangian. Similar to the type-I seesaw, the mass matrix for light neutrinos can be written as:

$$M_\nu = M_D M_R^{-1} M_D^T \tag{5.5}$$

where, $m_D =< \eta > y$ and $< \eta >= v$.

In our work, we extend the ν2HDM[71] by a gauge singlet fermion (S). The main motivation of this extended field is to incorporate dark matter phenomenology in our model. Furthermore, a flavor symmetric realization of this extension of ν2HDM is done with the help discrete flavour symmetries A_4 and Z_8. Non-Abelian discrete flavor symmetries play important role in model building[160, 71, 295]. A_4 being the discrete symmetry group of rotation leaving a tetrahedron invariant. It has 12 elements and 4 irreducible representation denoted by 1, $1'$, $1''$ and 3.

Along with the particle content of our model in addition to the SM particles (i.e three right handed neutrinos (N_1, N_2, N_3), one Higgs doublet (η) and one additional gauge singlet (S), we also introduce three sets of flavon fields φ, ξ and χ. Here, we have assigned left-handed lepton doublet (ℓ) to transform as A_4 triplet whereas right-handed charged leptons (e^c, μ^c, τ^c)

transform as 1, $1''$ and $1'$ respectively. An extra discrete symmetry Z_8 has been introduced in order to distinguish the neutrino and the flavon fields.

The particle content and charge assignments are shown in table (5.1).

Field	ℓ	e_R	μ_R	τ_R	H	η	φ	φ'	φ''	ξ	ξ'	χ	N_1	N_2	N_3	S
SU(2)	2	1	1	1	2	2	1	1	1	1	1	1	1	1	1	1
A_4	3	1	$1''$	$1'$	1	1	3	3	3	1	$1'$	1	1	$1'$	1	1
Z_8	ω^3	ω^4	ω^4	ω^4	ω^2	ω	ω^7	ω^2	ω^3	ω^6	ω^4	ω	ω^5	ω^2	ω	ω^2

Table 5.1 Particle content and their charge assignments under $SU(2)$, A_4 and Z_8 group.

Field	ζ	ζ'	ζ''
A_4	3	3	3
Z_8	ω^7	ω^2	ω^3

Table 5.2 Charge assignment of singlet flavons under A_4 and Z_8.

The leading order invariant Yukawa Lagrangian for the lepton sector is given by,

$$\mathcal{L} = \mathcal{L}_{M_l} + \mathcal{L}_{M_D} + \mathcal{L}_{M_R} + \mathcal{L}_{M_S} + h.c. \tag{5.6}$$

where,

$$\mathcal{L}_{M_l} = \frac{y_e}{\Lambda}(\bar{l}H\varphi)_{\underline{1}}e_R + \frac{y_\mu}{\Lambda}(\bar{l}H\varphi)_{\underline{1'}}\mu_R + \frac{y_\tau}{\Lambda}(\bar{l}H\varphi)_{\underline{1''}}\tau_R \tag{5.7}$$

$$\mathcal{L}_{M'_D} = \frac{y_1}{\Lambda}(\bar{l}\tilde{\eta}\varphi)_{\underline{1}}N_1 + \frac{y_2}{\Lambda}(\bar{l}\tilde{\eta}\varphi')_{\underline{1''}}N_2 + \frac{y_3}{\Lambda}(\bar{l}\tilde{\eta}\varphi'')_{\underline{1}}N_3 \tag{5.8}$$

$$\mathcal{L}_{M_R} = \frac{1}{2}\lambda_1\xi\bar{N^c}_{R_1}N_1 + \frac{1}{2}\lambda_2\xi'\bar{N^c}_{R_2}N_2 + \frac{1}{2}\lambda_3\xi\bar{N^c}_{R_3}N_3 \tag{5.9}$$

$$\mathcal{L}_{M_S} = \frac{1}{2}\rho\chi S^c N_1 \tag{5.10}$$

where Λ denotes the cut-off scale. To generate the desired light neutrino mas matrix we choose the vev alignments of the extra flavons as following,

$$< \varphi >= (\kappa,0,0) \, , < \varphi' >=< \varphi'' >= (\kappa,\kappa,\kappa) \, , < \xi >=< \xi' >= \kappa \, , < \chi >= u$$

Following the A_4 product rules[295] and using the above mentioned vev alignment, we can obtain the charged lepton mass matrix as follows

$$M_l = \frac{< H > \kappa}{\Lambda} \begin{pmatrix} y_e & 0 & 0 \\ 0 & y_\mu & 0 \\ 0 & 0 & y_\tau \end{pmatrix} \tag{5.11}$$

The Dirac mass matrix is given by,

$$M'_D = \begin{pmatrix} a & b & c \\ 0 & b & c \\ 0 & b & c \end{pmatrix} \tag{5.12}$$

The right handed neutrino mass matrix is,

$$M_R = \begin{pmatrix} M_1 & 0 & 0 \\ 0 & M_2 & 0 \\ 0 & 0 & M_3 \end{pmatrix} . \tag{5.13}$$

And the sterile neutrino mass matrix M_S can be written as,

$$M_S = \begin{pmatrix} s & 0 & 0 \end{pmatrix} \tag{5.14}$$

where, $a = \frac{<\eta>\kappa}{\Lambda} y_1$, $b = \frac{<\eta>\kappa}{\Lambda} y_2$, $c = \frac{<\eta>\kappa}{\Lambda} y_3$, M_1=$\lambda_1 \kappa$, M_2=$\lambda_2 \kappa$, M_3=$\lambda_3 \kappa$ and $s = \rho u$. Considering these M'_D, M_R and M_S in the light neutrino mass matrix[97]

$$M_\nu^{3\times 3} \simeq M'_D M_R^{-1} M_S^T (M_S M_R^{-1} M_S^T)^{-1} M_S (M_R^{-1})^T M_D'^T - M'_D M_R^{-1} M_D'^T \tag{5.15}$$

, we get;

$$M_\nu^{3\times 3} = \begin{pmatrix} -\frac{b^2}{M_2} - \frac{c^2}{M_3} & -\frac{b^2}{M_2} - \frac{c^2}{M_3} & -\frac{b^2}{M_2} - \frac{c^2}{M_3} \\ -\frac{b^2}{M_2} - \frac{c^2}{M_3} & -\frac{b^2}{M_2} - \frac{c^2}{M_3} & -\frac{b^2}{M_2} - \frac{c^2}{M_3} \\ -\frac{b^2}{M_2} - \frac{c^2}{M_3} & -\frac{b^2}{M_2} - \frac{c^2}{M_3} & -\frac{b^2}{M_2} - \frac{c^2}{M_3} \end{pmatrix} \tag{5.16}$$

It is clear that this matrix is a symmetric matrix generated by M_D', M_R and M_S matrices. It can produce only one mixing angle and one mass square difference. This symmetry must be broken in order to generate two mass square differences and three mixing angles. In order to introduce $\mu - \tau$ asymmetry in the light neutrino mass matrix we introduce $SU(2)_L$ singlet flavon fields ζ, $\zeta^{'}$ and $\zeta^{''}$ which breaks the μ-τ symmetric after being incorporated in the Dirac mass matrix (M_D'). This additional matrix has a crucial role to play in reproducing non-zero reactor mixing angle. And the Lagrangian responsible for generating the matrix can be written as,

$$\mathcal{L}_{M_P} = \frac{y_1}{\Lambda}(\bar{l}\tilde{\eta}\,\zeta)_{\underline{1}} N_1 + \frac{y_2}{\Lambda}(\bar{l}\tilde{\eta}\,\zeta')_{\underline{1''}} N_2 + \frac{y_3}{\Lambda}(\bar{l}\tilde{\eta}\,\zeta'')_{\underline{1}} N_3. \tag{5.17}$$

Taking vev alignment for the new flavon field as: $<\zeta>=<\zeta'>=<\zeta^{'}>=(0,\kappa,0)$, we get the matrix as,

$$M_P = \begin{pmatrix} 0 & 0 & p \\ 0 & p & 0 \\ p & 0 & 0 \end{pmatrix}. \tag{5.18}$$

Hence M_D takes the new form as,

$$M_D = M_D' + M_P = \begin{pmatrix} a & b & c+p \\ 0 & b+p & c \\ p & b & c \end{pmatrix}. \tag{5.19}$$

Therefore, we modify the light neutrino mass matrix by replacing M_D' by M_D which results in

$$M_\nu^{3\times 3} \simeq M_D M_R^{-1} M_S^T (M_S M_R^{-1} M_S^T)^{-1} M_S (M_R^{-1})^T M_D^T - M_D M_R^{-1} M_D^T. \tag{5.20}$$

The final light neutrino mass matrix is thus given by:

$$M_\nu^{3\times3} = \begin{pmatrix} -\frac{b^2}{M_2} - \frac{(c+p)^2}{M_3} & -\frac{-b(b+p)}{M_2} - \frac{c(c+p)}{M_3} & -\frac{b^2}{M_2} - \frac{c(c+p)}{M_3} \\ -\frac{-b(b+p)}{M_2} - \frac{c(c+p)}{M_3} & -\frac{c^2}{M_2} - \frac{(b+p)^2}{M_3} & -\frac{c^2}{M_2} - \frac{b(b+p)}{M_3} \\ -\frac{b^2}{M_2} - \frac{c(c+p)}{M_3} & -\frac{c^2}{M_2} - \frac{b(b+p)}{M_3} & -\frac{b^2}{M_2} - \frac{c^2}{M_3} \end{pmatrix}. \tag{5.21}$$

The 4×4 active sterile neutrino mass matrix represented as in eq.(5.1) becomes,

$$M_\nu^{4\times4} = \begin{pmatrix} -\frac{a^2}{M_1} - \frac{b^2}{M_2} - \frac{(c+p)^2}{M_3} & -\frac{b(b+p)}{M_2} - \frac{c(c+p)}{M_3} & -\frac{b^2}{M_2} - \frac{ap}{M_1} - \frac{c(c+p)}{M_3} & -\frac{as}{M_1} \\ -\frac{b(b+p)}{M_2} - \frac{c(c+p)}{M_3} & -\frac{c^2}{M_3} - \frac{(b+p)^2}{M_2} & -\frac{c^2}{M_3} - \frac{b(b+p)}{M_2} & 0 \\ -\frac{b^2}{M_2} - \frac{ap}{M_1} - \frac{c(c+p)}{M_3} & -\frac{c^2}{M_3} - \frac{b(b+p)}{M_2} & -\frac{b^2}{M_2} - \frac{c^2}{M_3} - \frac{p^2}{M_1} & -\frac{ps}{M_1} \\ -\frac{as}{M_1} & 0 & -\frac{ps}{M_1} & \frac{s^2}{M_1} \end{pmatrix}. \tag{5.22}$$

In $M_\nu^{4\times4}$, there exists three eigenstates for three active neutrinos and one for the light sterile neutrino.

Since we have included one extra generation of neutrino along with the active neutrinos in our model thus, the final neutrino mixing matrix for the active-sterile mixing takes 4×4 form as[97],

$$V \simeq \begin{pmatrix} (1-\frac{1}{2}RR^\dagger)U_{PMNS} & R \\ -R^\dagger U_{PMNS} & 1-\frac{1}{2}RR^\dagger \end{pmatrix} \tag{5.23}$$

where $R = M_D M_R^{-1} M_S^T (M_S M_R^{-1} M_S^T)^{-1}$ is a 3×1 matrix representing the strength of active sterile mixing and U_{PMNS} is the leptonic mass matrix for active neutrinos given by eq.(1.24).

5.3 Sterile Dark Matter

A minimally extended Standard Model of particle physics can easily accommodate a non resonantly produced sterile dark matter. With the mass of sterile neutrino restricted to a few keV, it can be considered as a prime candidate for warm DM. The sterile neutrinos couples with the standard model particles only via its mixing to the active neutrinos. Thus,

from the active neutrinos which are a part of the primordial plasma (as they are weakly interacting), the DM abundance can be eventually build up. This mechanism is also known as the Dodelson and Widrow (DW) mechanism. The non resonant production (NPR) of sterile neutrinos takes place in absence of lepton asymmetry. However, for compelling amount of lepton asymmetry in the primordial plasma, we can get resonant sterile neutrinos having very small mixing angles and thereby producing notable colder momenta. This production mechanism is also known as Shi & Fuller (SF) or resonant production mechanism[299]. A minimum amount of dark matter contribution which can be produced as a consequence of the dark matter mass and the mixing angle is accounted by non resonant production mechanism. In our model, we have considered a singlet sterile fermion (S) which acts as a non resonant DM candidate. Thus, from now on we denote the sterile fermion mass as m_{DM}. We solve the model parameters with some fixed values of variables such as M_1, M_2 and M_3 in the range $10^4 - 10^5$ GeV, $5 \times 10^5 - 10^6$ GeV and $10^7 - 10^8$ GeV respectively. Also the lightest of the active neutrinos is considered very small having mass in the range $10^{-10} - 10^{-9}$ eV. On computing these values we are able to get the desired mass m_{DM}, i.e. in keV range and also the mixing angle $sin^2(2\theta_{DM})$ satisfying the cosmological bounds. In our work, the contribution towards the mixing angles comes from V_{14} and V_{34}, non-vanishing components of the mixing matrix V (5.23). The relic abundance of any species can be expressed as[294],

$$\Omega_x h^2 = \frac{\rho_{x_0}}{\rho_{crit}} = \frac{s_0 Y_\infty m}{\rho_{crit}} \tag{5.24}$$

where, ρ_{x_0} is present energy density of x, ρ_{crit} represents the critical energy density of the universe, s_0 is the present day entropy and Y_∞ is the present abundance of the particle x. Also we can get the values of $\rho_{crit} \approx 1.054 * 10^{-5} h^2 GeV\, cm^{-3}$ and $s_0 \approx 2886 cm^{-3}$ from Particle Data Group (PDG).

Further in case of sterile neutrinos, it can be expressed by the relation:[293]

$$\Omega_{\alpha x} = \frac{m_x Y_{\alpha x}}{3.65 \times 10^{-9} h^2 GeV}. \tag{5.25}$$

where $\alpha = e, \mu, \tau$.

Now the resulting relic abundance of any sterile neutrino state with a non-vanishing mixing to the active neutrinos, is proportional to the active-sterile mixing and the mass of the sterile, which is again expressed as[296, 297],

$$\Omega_{\alpha S} h^2 = 1.1 \times 10^7 \sum C_\alpha(m_s) |V_{\alpha s}|^2 (\frac{m_s}{keV})^2 \tag{5.26}$$

where,

$$C_\alpha(m_s) = 2.49 \times 10^{-5} \frac{Y_{\alpha s} keV}{sin^2(\theta_{\alpha s}) m_s}. \tag{5.27}$$

C_α are active flavor dependent coefficients and can be neumerically computed by solving Boltzman equation[290].

Using the parametrisation $|V_{\alpha s} \simeq Sin(\theta_{\alpha s})|$ and with the consideration of sterile neutrino as a dark matter candidate, we replace the symbol s by DM in the following expression for relic abundance. Therefore, the simplified equation for relic abundance for non resonantly produced dark matter takes the form[289–292]:

$$\Omega_{DM} h^2 \simeq 0.3 \times 10^{10} sin^2(2\theta_{DM}) (\frac{m_{DM} \times 10^{-2}}{keV})^2 \tag{5.28}$$

where, Ω_{DM} is directly proportional to m_{DM} which is the DM mass as mentioned earlier and $sin^2(2\theta_{DM})$ viz the active-DM mixing angle with $sin^2(2\theta_{DM}) = 4(V_{14}^2 V_{34}^2)$.

5.3.1 Constraints on non resonant sterile dark matter

The decay rate of a sterile neutrino when it radiatively decays into an active neutrino and a photon γ with its energy $E_\gamma = \frac{m_{DM}}{2}$ is strictly dependent on dark matter mass. Thus, sterile

neutrinos bearing masses above the keV range is significantly ruled out under the above mentioned condition. The decay rate for the process $S \longrightarrow \nu + \gamma$ is given by[267]:

$$\Gamma \simeq 1.38 \times 10^{-22} sin^2(2\theta_{DM}) \left(\frac{m_{DM}}{keV}\right)^5 s^{-1}. \tag{5.29}$$

For a particle to be a DM candidate, one of the crucial conditions is its stability. Thus, despite the probable decay of the sterile neutrino, it can be considered as a DM candidate due to the negligible decay rate of S as a consequence of the mixing angles.

A significant experimental observation which can be considered for analysing cosmology is the Lyman-α observations. Based on this Lyman-α observation, various studies over the past decade have put forward constraints on the non-resonant sterile neutrino DM. The constraints obtained are applicable to thermal relic WDM as they are equivalent to non-resonant sterile DM and thus, we can find a conversion relation between non-resonant sterile DM mass(m_{nrs}) and thermal relic WDM mass (m_{WDM})[266]. Thermal relic masses below 0.75 keV (approx) was ruled out earlier in[268], however, later a more stringent bound was found by[269] of $m_{WDM} \geq 2.5$ keV. The latter constraint was based on the SDSS data, which permitted to exclude non-resonantly produced sterile neutrinos as probable DM candidate. Again, a few years back a 2σ limit on $m_{WDM} \geq 3.3$ keV corresponding to $m_{nrs} \geq 18.5$ keV was recounted by[270]. Recent works could give more tighter bounds as they used more than 13000 quasar spectra from the BOSS survey. It therefore, reported a 2σ limit of $m_{WDM} \geq 4.35$ keV (corresponding to $m_{nrs} \geq 26.4$ keV[298]). The analysis done by[266] shows that the Milky-way satellite counts discards models wherein the particle mass is below $m_{DM} \sim 4.5$ keV and larger region of higher order masses. This allows the parameter space near around the line signal, i.e $m_{DM} = 7.1$ keV. Again, from V13 model based Lyman-α limit and X-ray bounds, a narrow area above $m_{DM} \sim 10$ keV remains allowed. Interestingly, the generalised Lyman-α bound coming from B15 reference model thoroughly overlaps with the Suzaku X-ray limits , thereby, disfavouring the entire regime of resonantly produced

sterile neutrino DM. Thus, a very significantly robust limit is drawn for both non-resonant and resonant production of sterile neutrino.

5.4 Leptogenesis

We study baryogenesis in neutrino two Higgs doublet model realised by $A_4 \times Z_8$ symmetry. Leptogenesis[67] is the process by which the observed baryon asymmetry of the Universe(BAU) can be produced.

In the beyond standard model, the right handed neutrino with the lightest mass decays to a Higgs doublet and a lepton doublet. The Majorana property of the neutrino produces a significant amount of lepton asymmetry in the decay process. The standard model Lagrangian conserves both lepton number and baryon numbers. But chiral anomalies in BSM theories results in violation in $(B+L)$ while conserving $(B-L)$.

The lepton asymmetry is generated by the out-of- equilibrium CP-violating decays of right hand neutrino, in our case N_1. As discussed in many literatures[86, 221], we now know that there exists a lower bound of about 10 TeV for the lightest of the RHNs (M_1) considering the vanilla leptogenesis scenario[68, 35].

For a hierarchical mass of RHN, i.e $M_1 << M_2, M_3$, the leptogenesis produced by the decay of N_2 and N_3 are suppressed due to the strong washout effects produced by N_1 or N_2 and N_3 mediated interactions[35]. Thereby, the lepton asymmetry is produced only by the virtue of N_1 decay and the lepton asymmetry can be converted to baryon asymmetry via violation of $(B+L)$ through the process known as 'sphalerons'.[222]. Now for the generation of BAU, we solve the simultaneous Boltzmann equations for N_1 decay and formation of N_{B-L}. For producing lepton asymmetry, the decay rate for lepton number violating processes associated with particles and antiparticles must be different. The B-L calculation depends on

the comparison between the decay rates for $N_1 \to l\eta, \bar{l}\eta^*$ processes and the Hubble parameter, which causes a certain impact on the asymmetry as well as on the CP-asymmetry parameter ε_1. In the calculation of leptogenesis, one important quantity that differentiates between weak and strong washout regime is the decay parameter and is expressed as eq.(1.52). Again the expression for Hubble parameter H used in the decay parameter equation is given by eq.(2.21). We consider the RHN masses as $M_1 = 10^4 - 10^5$ GeV, $M_2 = 5 \times 10^5 - 10^6$ GeV and $M_3 = 10^7 - 10^8$ GeV. Now, by this choice of RHN masses along with $m_{\eta_R^0} = 1 - 10$ GeV and most significantly the lightest active neutrino mass $m_l = 10^{-10} - 10^{-9}$ eV, we fall on the weak washout regime. The Yukawa couplings obtained by solving the model parameters are incorporated in the decay rate equation for N_1 which is given by,

$$\Gamma_1 = \frac{M_1}{8\pi}(Y^\dagger Y)_{11}\left[1 - \left(\frac{m_{\eta_R^0}}{M_1}\right)^2\right]^2 = \frac{M_1}{8\pi}(Y^\dagger Y)_{11}(1-\eta_1)^2 \tag{5.30}$$

Again for the decays $N_1 \to l\eta, \bar{l}\eta^*$, the CP asymmetry parameter ε_1 is given by,

$$\varepsilon_1 = \frac{1}{8\pi(Y^\dagger Y)_{11}}\sum_{j\neq 1} Im[(Y^\dagger Y)^2]_{1j}\left[f(r_{j1},\eta_1) - \frac{\sqrt{r_{j1}}}{r_{j1}-1}(1-\eta_1)^2\right], \tag{5.31}$$

where,

$$f(r_{j1},\eta_1) = \sqrt{r_{j1}}\left[1 + \frac{(1-2\eta_1+r_{j1})}{(1-\eta_1)^2} ln\left(\frac{r_{j1}-\eta_1^2}{1-2\eta_1+r_{j1}}\right)\right], \tag{5.32}$$

and $r_{j1} = \left(\frac{M_j}{M_1}\right)^2$, $\eta_1 \equiv \left(\frac{m_{\eta_R^0}}{M_1}\right)^2$.

The Yukawa couplings participating in eq.(5.31) are obtained from the model on solving the model parameters. The Boltzmann equations for the number densities of N_1 and N_{B-L}, given by[86],

$$\frac{dn_{N_1}}{dz} = -D_1(n_{N_1} - n_{N_1}^{eq}), \tag{5.33}$$

$$\frac{dn_{B-L}}{dz} = -\varepsilon_1 D_1(n_{N_1} - n_{N_1}^{eq}) - W_1 n_{B-L}, \tag{5.34}$$

respectively. In eq.(5.33) and (5.34), the terms have their usual meaning as discussed in many literatures[35, 37]. The final $B-L$ asymmetry n^f_{B-L} is evaluated by numerically calculating eq.(5.33) and eq.(5.34) before the sphaleron freeze-out. This is converted into the baryon-to-photon ratio given by:

$$n_B = \frac{3}{4}\frac{g^0_*}{g_*} a_{sph} n^f_{B-L} \simeq 9.6 \times 10^{-3} n^f_{B-L}, \tag{5.35}$$

In eq.(5.35), $g_* = 106.75$ is the effective relativistic degrees of freedom at the time when final lepton asymmetry was produced, $g^0_* = \frac{43}{11}$ is the effective degrees of freedom at the recombination epoch and $a_{sph} = \frac{8}{23}$ is the sphaleron conversion factor taking two Higgs doublet into consideration. On solving the model parameters and incorporating in the equations responsible for generating BAU as mentioned in this section, we get quite satisfactory results abiding the Planck limit viz $(6.04 \pm 0.08) \times 10^{-10}$[210] .

5.5 Numerical analysis and results

The leptonic mixing matrix for active neutrinos depends on three mixing angles θ_{13}, θ_{23} and θ_{12} and one CP-violating phase (δ) for Dirac neutrinos and two Majorana phases ϕ_1 and ϕ_2 for Majorana neutrino. The Leptonic mass matrix for active neutrino is parameterized as,

$$U_{PMNS} = \begin{pmatrix} c_{12}c_{13} & s_{12}c_{13} & s_{13}e^{-i\delta} \\ -s_{12}c_{23} - c_{12}s_{23}s_{13}e^{i\delta} & c_{12}c_{23} - s_{12}s_{23}s_{13}e^{i\delta} & s_{23}c_{13} \\ s_{12}s_{23} - c_{12}c_{23}s_{13}e^{i\delta} & -c_{12}s_{23} - s_{12}c_{23}s_{13}e^{i\delta} & c_{23}c_{13} \end{pmatrix} .P \tag{5.36}$$

Here $c_{ij} = cos\theta_{ij}$, $s_{ij} = sin\theta_{ij}$ and P would be a unit matrix in the Dirac case but in Majorana case $P = diag(e^{\frac{i\phi_1}{2}}, 1, e^{\frac{i\phi_2}{2}})$

The light neutrino mass matrix is diagonalized by the unitary PMNS matrix as,

$$M_\nu^{3\times 3} = U_{PMNS} \cdot diag(m_1, m_2, m_3) \cdot U^T_{PMNS} \tag{5.37}$$

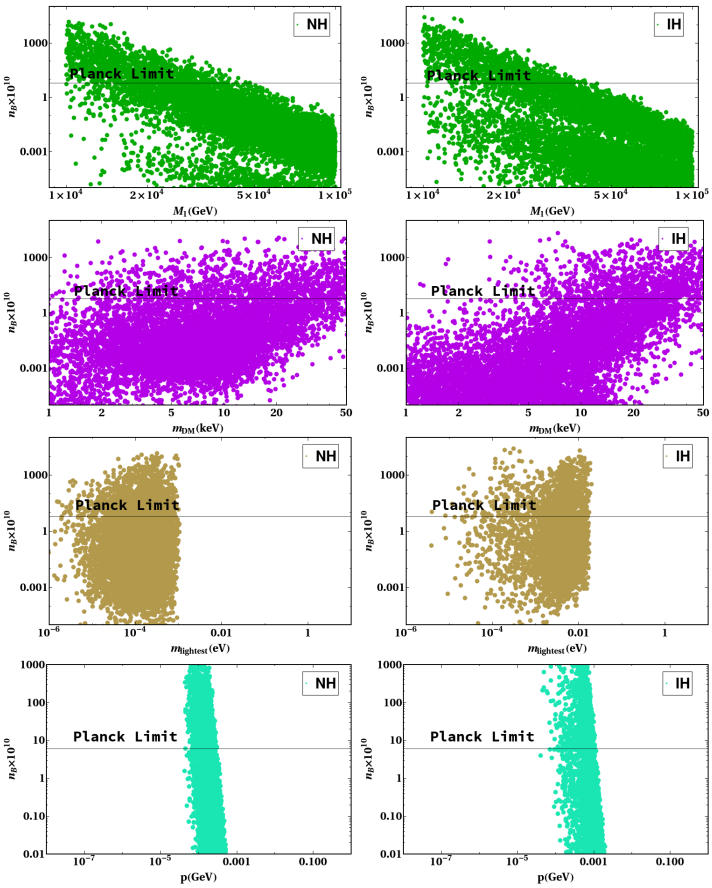

Fig. 5.1 Plots in the first-row shows baryon asymmetry as a function of RHN (M_1), the second-row shows baryon asymmetry as a function of dark matter mass(M_{DM}), in third-row baryon asymmetry as a function of lightest neutrino mass eigenvalue(m_l) is depicted and in the fourth row we show a plot between perturbation(p) and BAU respectively. The black horizontal line gives the current Planck limit for BAU viz. 6.05×10^{-10}.

where m_1, m_2 and m_3 are three active neutrino masses.

Since we have included one extra generation of neutrino along with the active neutrinos in our model thus, the final neutrino mixing matrix for the active-sterile mixing takes 4×4 form as,

$$V \simeq \begin{pmatrix} (1-\frac{1}{2}RR^{\dagger})U_{PMNS} & R \\ -R^{\dagger}U_{PMNS} & 1-\frac{1}{2}RR^{\dagger} \end{pmatrix} \tag{5.38}$$

where $R = M_D M_R^{-1} M_S^T (M_S M_R^{-1} M_S^T)^{-1}$ is a 3×1 matrix representing the strength of active sterile mixing.

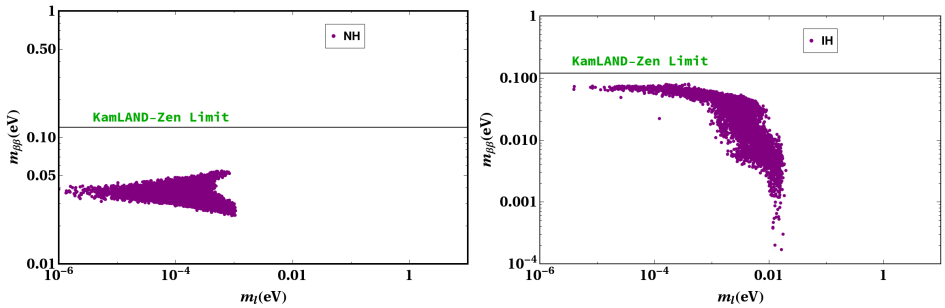

Fig. 5.2 Lightest active neutrino mass(m_l) as a function of effective mass($m_{\beta\beta}$) for NH/IH. The horizontal(black) line depicts the upper bound on the effective mass ($m_{\beta\beta}(eV) \sim 0.12(eV)$) of light neutrinos obtained from KamLAND-Zen experiment.

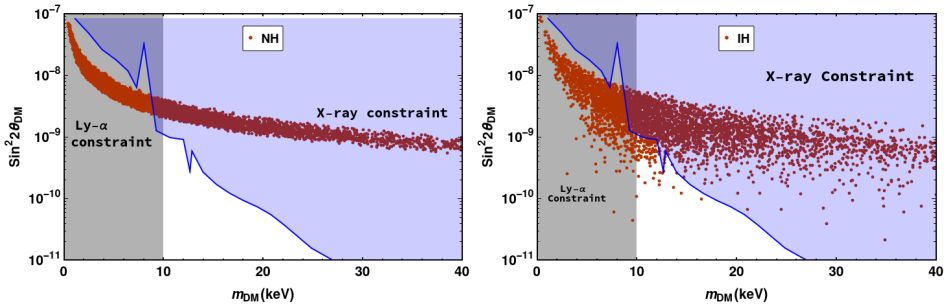

Fig. 5.3 Plot between dark matter mass(m_{DM}) and active-DM mixing angle including constraints from Lyman-α and X-ray for NH/IH.

Now the active-sterile neutrino mass matrix can be diagonalized by the mixing matrix, V as,

$$M_\nu^{4\times4} = V \cdot diag(m_1, m_2, m_3, m_4) \cdot V^T \tag{5.39}$$

The sterile mass is obtained from eq.(5.3) as:

$$m_s = \frac{s^2}{M_1}, \tag{5.40}$$

which is considered as the dark matter mass and is represented as m_{DM} in our analysis.

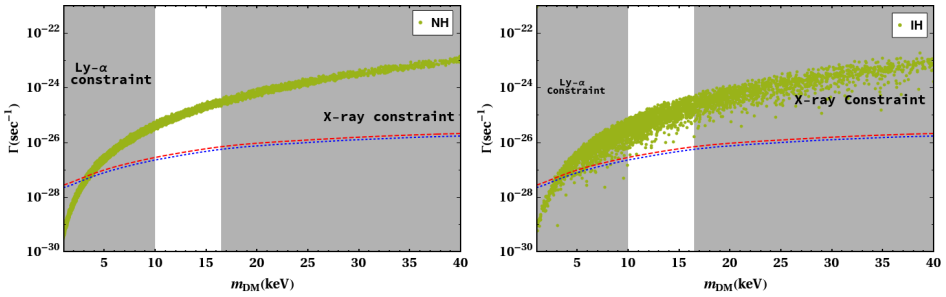

Fig. 5.4 Plot between dark matter mass(m_{DM}) and decay rate for the process $S \longrightarrow \nu + \gamma$ including constraints from Lyman-α and X-ray for NH/IH. We also give lifetime constraint of sterile neutrinos as a function of mass. The red dashed (blue dotted) line represents the case when energy transfer from CMB photons to gas is included (excluded).

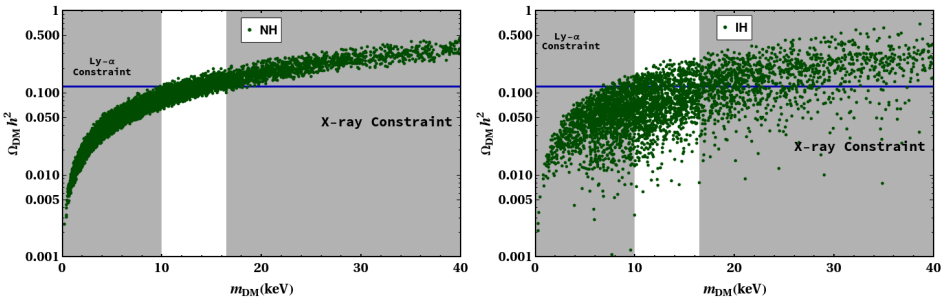

Fig. 5.5 Variation between dark matter mass and relic abundance with the constraints obtained from Lyman-α and X-ray for NH/IH.

5.5.1 Neutrinoless double beta decay

A very important open problem in neutrino physics is the search for true nature of neutrino whether its Dirac particle or Majorana particle. From the theoretical point of view it is expected that neutrinos are Majorana particles (the necessity of extremely small values of the neutrino Yukawa coupling constants is commonly considered as a strong argument against a SM origin of the neutrino masses). Neutrinoless double beta decay ($0\nu\beta\beta$) is one of the lepton number violating processes which can probe Majorana nature of neutrino.

$$(A,Z) \longrightarrow (A,Z+2) + e^- + e^- \tag{5.41}$$

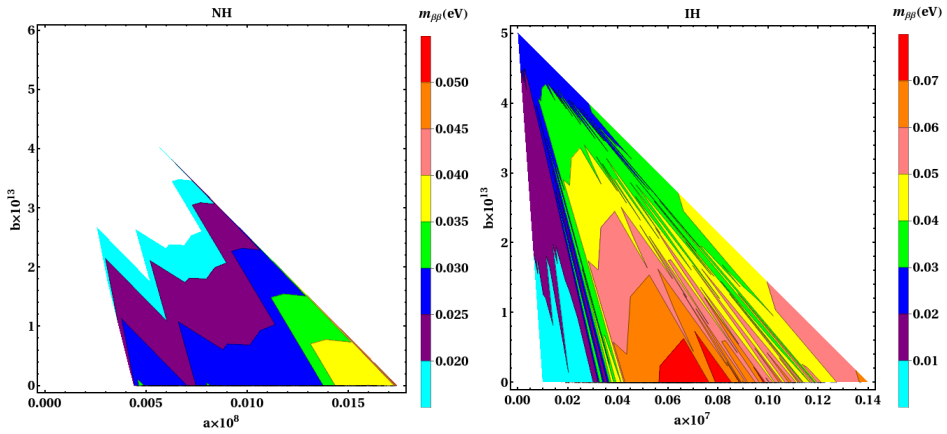

Fig. 5.6 Contour plot showing the parameter space of model parameters a and b w.r.t effective mass($m_{\beta\beta}$) for NH/IH.

Free Parameter	NH/IH
$M_1(GeV)$	10^4 - 10^5
$M_2(GeV)$	5×10^5 - 10^6
$M_3(GeV)$	10^7 - 10^8
$m_l(eV)$	10^{-10} - 10^{-9}
$s(GeV)$	0.1 - 1

Table 5.3 Range of the free parameters.

whose amplitude is proportional to the effective Majorana mass,

$$\mid m_{\beta\beta} \mid = \mid \sum_k V_{ek}^2 m_k \mid \tag{5.42}$$

where V is the active-sterile mixing matrix.

Using the standard parameterization of the $(3+1)$ active-sterile mixing matrix, the effective Majorana mass in $0\nu\beta\beta$ decay can be written as

$$\mid m_{\beta\beta} \mid = \mid c_{13}^2 c_{12}^2 c_{14}^2 m_1 e^{i\phi_1} + c_{13}^2 s_{12}^2 c_{14}^2 m_2 + s_{13}^2 c_{14}^2 m_3 e^{i\phi_2} + s_{14}^2 m_4 \mid \tag{5.43}$$

The parameters involved are:

(i) the angles θ_{12} and θ_{13}, measured with good precision by the solar, short-baseline reactor

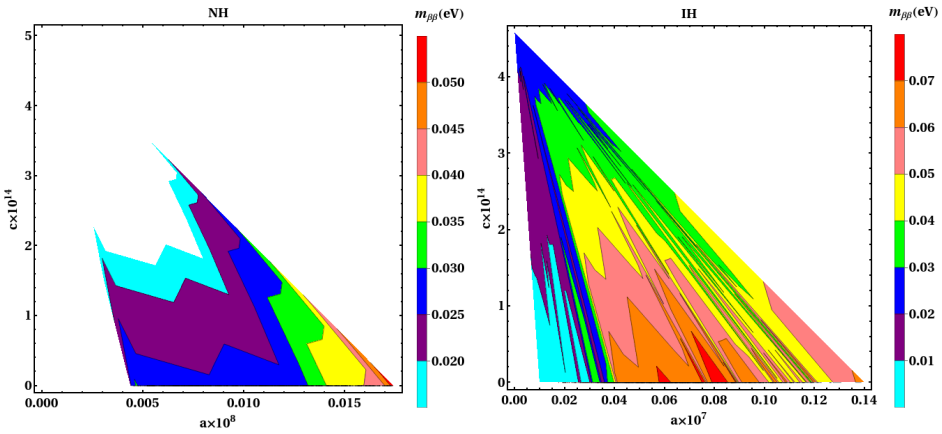

Fig. 5.7 Contour plot showing the parameter space of model parameters a and c w.r.t effective mass($m_{\beta\beta}$) for NH.

Model Parameter	NH (eV)	IH (eV)
a	0.005×10^8-0.015×10^8	0.02×10^7- 0.14×10^7
b	0.1×10^{13}-3.5×10^{13}	0.1×10^{13} -5×10^{13}
c	0.1×10^{14}-3×10^{14}	0.1×10^{14}-4.6×10^{14}
p	0.1×10^6-0.5×10^6	0.01×10^7- 0.2×10^7

Table 5.4 Allowed range of the model parameters satisfying effective mass

neutrino experiments, respectively;

(ii) the neutrino mass eigenstates m_1 , m_2, m_3 and m_4 , which are related to the solar (Δm^2_S), atmospheric (Δm^2_A) and LSND (Δm^2_{LSND}) squared mass differences :

$$\Delta m^2_S = \Delta m^2_{12} \tag{5.44}$$

$$\Delta m^2_A = \frac{1}{2} \mid \Delta m^2_{13} + \Delta m^2_{23} \mid \tag{5.45}$$

$$\Delta m^2_{LSND} = \Delta m^2_{41} or \Delta m^2_{43} \tag{5.46}$$

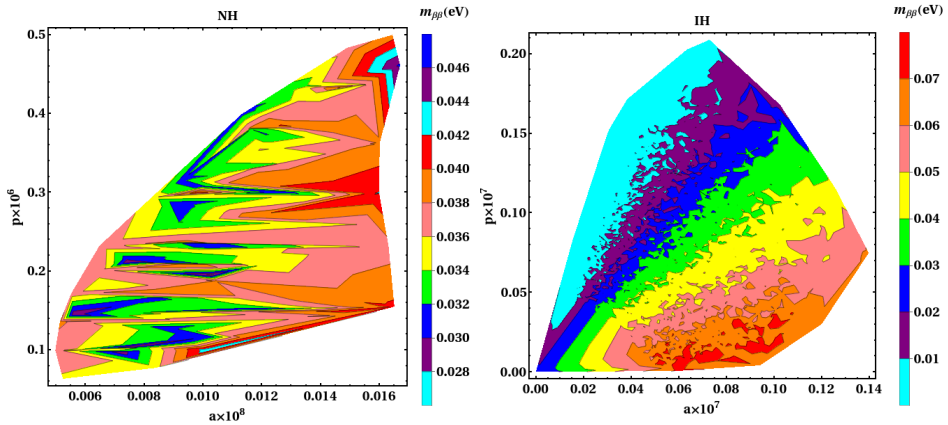

Fig. 5.8 Contour plot showing the parameter space of model parameters a and p w.r.t effective mass($m_{\beta\beta}$) for NH/IH.

The relation between the mass eigenstates and the squared mass differences allows two possible orderings of the neutrino masses :

Normal mass hierarchy : $(m_1 \ll m_2 < m_3 \ll m_4)$

$$m_1 = m_{min},\ m_2 = \sqrt{m_{min}^2 + \Delta m_S^2},\ m_3 = \sqrt{m_{min}^2 + \Delta m_A^2 + \frac{\Delta m_S^2}{2}},\ m_4 = \sqrt{m_{41}^2}$$

Inverted mass hiearchy : $(m_3 \ll m_1 < m_2 \ll m_4)$

$$m_{min} = m_3,\ m_1 = \sqrt{m_{min}^2 + \Delta m_A^2 - \frac{\Delta m_S^2}{2}},\ m_2 = \sqrt{m_{min}^2 + \Delta m_A^2 + \frac{\Delta m_S^2}{2}},\ m_4 = \sqrt{m_{43}^2}.$$

5.5.2 Results

A cumulative study has been carried out in this flavor symmetric ν2HDM so as to have a wider perspective on the viability of the model. The choice of free parameters considered in our work is given in table (5.3). The entire work is carried out keeping these benchmark parameter space fixed. From fig.(5.1), we obtain variational plots between baryon asymmetry of the Universe calculated from the model and the free parameters considered in our work except for the plot in the last row. We have chosen a diagonal perturbation matrix in order to break the $\mu - \tau$ symmetry of the neutrino mass matrix, thus, in last row of fig.(5.1) we show the parameter space of perturbation(p) satisfying the Planck limit for BAU. We find

only a narrow region of space ranging from $10^{-4} - 10^{-3}$ GeV which have points obeying constraints for BAU in case of both NH/IH. Also the range of RHN mass corresponding to Planck limit for both the hierarchies are same, i.e. $10^4 - 5 \times 10^4$ GeV as shown in first row of fig.(5.1). However, there is a difference in the allowed parameter space for dark matter mass. For NH, the entire DM mass range $1 - 50$ keV satisfies the BAU bound whereas in case of IH, we have distinct allowed points in the range $5 - 50$ keV. The lightest active neutrino mass is also constrained in our work, wherein the allowed range for NH is approximately $10^{-5} - 10^{-3}$ eV and that for IH is $10^{-4} - 10^{-2}$ eV. In fig.(5.2), both NH and IH satisfies the KamLAND-Zen limit for effective mass in variation with m_l. As discussed in sec.(3.2), the Lyman-α bound on m_{DM} forbids mass below 10 keV in case of non resonantly production of sterile neutrino (which serve as a DM candidate in our case). Results of dark matter phenomenology is discussed in the points below:

• Fig.(5.3) shows a co-relation between dark matter mass and active-DM mixing angle. A very small region between $10 - 16$ keV falls in the allowed parameter space for IH whereas the entire parameter space for NH falls in the excluded region.

• We have also shown a plot of dark matter mass w.r.t the decay rate (Γ) for both NH and IH respectively in fig.(5.4). The allowed space consists of points corresponding to dark matter mass $10 - 16$ keV in context with the bounds coming from Lyman-α and X-ray for both NH and IH. Though we have shown the variation plot of m_{DM} vs. Γ, but the mass region for NH is not allowed as obtained from fig.(5.3). We have also taken into account constraints from lifetime of sterile neutrinos w.r.t its mass. As can be seen from fig.(5.4), the red dashed line corresponds to the upper bound coming from lifetime of sterile neutrinos for the case when energy transfer from cosmic microwave background (CMB) photons to gas is included and the blue dotted lines is for the case when this very energy is exluded. Considering this constraint, the results obtained excludes all the points for NH, whereas for IH, we have very scanty points in the boundary of 10 keV which tends to satisfy the lifetime bounds.

• Similarly in fig.(5.5), we have shown the dark matter mass range which obeys the Planck limit for relic abundance of dark matter. In case of NH, $m_{DM} = 10 - 16$ keV satisfies the stringent bound for relic abundance though this region is disallowed from fig.(5.3). We have larger number of points for IH in the allowed parameter space m_{DM}=10 − 16 keV satisfying the Planck bound.

fig.(5.6),(5.7) and (5.8) depicts the range of the model parameters a, b, c and the perturbation p consistent with the KamLAND-Zen limit for effective mass of neutrinos. A tabular form comprising of the allowed space of the model parameters is depicted in Table.(5.4).

We cannot comment on the more preferable hierarchy for neutrino phenomenology or baryon asymmetry of the Universe due to their identical allowed parameter space. However, in case of dark matter we can consider IH to have shown a wider range of parameter space when compared to NH which abide by the experimental or observational constants.

5.6 Summary

In our work we have studied neutrino phenomenology and related cosmology of an extension of ν2HDM realized with the help of $A_4 \otimes Z_8$ flavour symmetries. The particle content of our model includes three right handed neutrino fields (N_1, N_2, N_3), one Higgs doublet (η), one additional gauge singlet (S) and four sets of flavon fields $(\varphi, \xi, \chi, \zeta)$ to the Standard Model of particle physics. The Dirac mass matrix (M'_D), Majorana mass matrix (M_R), sterile mass matrix (M_S) are constructed as required using the A_4 product rules. A perturbation (M_P) is incorporated in the M'_D in order to break the $\mu - \tau$ symmetry in the light neutrino mass matrix to generate the non zero reactor mixing angle and obtain a 4×4 active-sterile mass matrix similar to the MES framework. We analyse both the normal and inverted hierarchies extensively in this work. The model parameters are solved comparing the active-sterile neutrino matrix diagonalised by the active-sterile mixing matrix in eq.(5.39). After evaluating the model parameters, the sterile neutrino mass(which is the Dark Matter

candidate) and DM-active mixing angle is calculated. In this work, we have considered non resonant production of sterile neutrino and thus the constraints from Lyman-α and X-ray are implemented accordingly. The variation of active-DM mixing angle with DM mass is studied and it is observed that the data points satisfy the Lyman-α and X-ray constraints in the IH case but are disfavored for NH. The decay rate of the DM for the process $S \longrightarrow \nu + \gamma$ is also calculated. We obtain a low decay rate which establishes the stability of the dark matter candidate in the cosmological scales. The relic abundance of the dark matter candidate is also checked and studied w.r.t the variation in DM mass. Also in this case, we see that the number of data points that satisfy the Lyman-α and X-ray constraints in IH are more than that compared to NH. Overall, the dark matter phenomenology is more compatible for IH. Baryogenesis is also studied in our work due to its crucial role in phenomenological analysis. In our model, BAU is generated through the out of equilibrium decay of $N_1 \rightarrow l\eta, \bar{l}\eta^*$, where N_1 is lightest right handed neutrino. We study baryon asymmetry as a function of lightest right handed neutrino mass (N_1), DM mass, lightest active neutrino mass and perturbation (p) considering constraints from Planck limit. We also calculate the effective neutrino mass and then study it's variation with lightest active neutrino mass and validate with KamLAND-Zen limit. The allowed parameter space of model parameters is generated w.r.t the effective mass of active neutrinos. In conclusion we can say that IH has shown a wider range of parameter space in case of dark matter compared to NH. An identical allowed parameter space in the both hierarchies is seen in neutrino phenomenology and BAU. Thus, we can consider our model to be consistent in addressing dark matter, neutrino phenomenology and baryon asymmetry of the universe simultaneously.